

UvA-DARE (Digital Academic Repository)**Conformational studies of ligand-template assemblies and the consequences for encapsulation of rhodium complexes and hydroformylation catalysis**

Jacobs, I.; van Duin, A.C.T.; Kleij, A.W.; Kuil, M.; Tooke, D.M.; Spek, A.L.; Reek, J.N.H.

Published in:
Catalysis Science & Technology

DOI:
[10.1039/c3cy20665c](https://doi.org/10.1039/c3cy20665c)

[Link to publication](#)

Citation for published version (APA):

Jacobs, I., van Duin, A. C. T., Kleij, A. W., Kuil, M., Tooke, D. M., Spek, A. L., & Reek, J. N. H. (2013). Conformational studies of ligand-template assemblies and the consequences for encapsulation of rhodium complexes and hydroformylation catalysis. *Catalysis Science & Technology*, 3(8), 1955-1963. <https://doi.org/10.1039/c3cy20665c>

General rights

It is not permitted to download or to forward/distribute the text or part of it without the consent of the author(s) and/or copyright holder(s), other than for strictly personal, individual use, unless the work is under an open content license (like Creative Commons).

Disclaimer/Complaints regulations

If you believe that digital publication of certain material infringes any of your rights or (privacy) interests, please let the Library know, stating your reasons. In case of a legitimate complaint, the Library will make the material inaccessible and/or remove it from the website. Please Ask the Library: <https://uba.uva.nl/en/contact>, or a letter to: Library of the University of Amsterdam, Secretariat, Singel 425, 1012 WP Amsterdam, The Netherlands. You will be contacted as soon as possible.

Cite this: *Catal. Sci. Technol.*, 2013, **3**, 1955

Conformational studies of ligand-template assemblies and the consequences for encapsulation of rhodium complexes and hydroformylation catalysis†

Ivo Jacobs,^a Adri C. T. van Duin,^b Arjan W. Kleij,^{‡a} Mark Kuil,^a Duncan M. Tooke,^c Anthony L. Spek^c and Joost N. H. Reek^{*a}

The second coordination sphere around a transition metal catalyst can contribute to the activity and selectivity that it displays. In this paper we present encapsulated catalysts using a template-ligand assembly strategy based on Zn(II)salphen building blocks, and show that these have significantly different properties in catalysis than previously reported Zn(II)porphyrin-based analogues. The conformational properties of tris-Zn(II)salphen-based capsular catalysts were examined by a combination of solid state and solution phase analytical methods, as well as computational techniques. We found that as a result of the ability of the salphen-based capsules to adopt different conformations compared to porphyrin-based capsules, less stringent constraints are enforced to the catalytic centre, resulting in different catalyst selectivities displayed by the rhodium complexes enclosed.

Received 24th September 2012,
Accepted 21st January 2013

DOI: 10.1039/c3cy20665c

www.rsc.org/catalysis

Introduction

Self-assembled molecular capsules with hollow structures can encapsulate smaller guest molecules within their cavities.¹ Since the 1990s, various research groups have investigated the application of such capsules as nanoreactors.² A diversity of chemical processes, both stoichiometric and catalytic, has been carried out within molecular capsules.³ Reactions can be accelerated, as shown for example by Raymond and coworkers. They demonstrated that acid-catalyzed reactions can be carried out inside nano-environments even if the outside conditions are basic.⁴ Also the selectivity of a chemical process can be changed completely, as shown by Fujita *et al.* in the Diels–Alder reaction⁵ and this particular example, where unique selectivities are obtained, shows the influential nature of the finite micro-environment within the capsule. Such unusual selectivities are

generally not achieved using traditional catalytic approaches. Although the field of supramolecular capsular catalysis is still in its developmental stage, several successful examples of reactions carried out within self-assembled nanoreactors have appeared and demonstrate the power of the concept. Detailed studies are required to fully understand the mechanisms behind the effects observed when carrying out reactions in these confined spaces.

We have previously reported a general strategy to encapsulate phosphine ligands and metal complexes thereof (Scheme 1).⁶ The strategy is based on template-ligands, which are building blocks that have one type of coordination site for the transition metal that is active in catalysis, and another type of coordination site used in the self-assembly of the capsule. Initially we used Zn(II)porphyrin building blocks for the assembly process. A tenfold increase in conversion and reversed regio-selectivity (*i.e.*, linear-branched ratio) was found when using **3a** in the rhodium catalysed hydroformylation of 1-octene. When using internal octenes, a fourfold increase in yield was found as well as unprecedented selectivity.⁷ In order to extend the diversity of the building blocks and to vary the size and/or shape of the catalytic capsules, we also used Zn(II)salphen.⁸ These are easier to prepare than Zn(II)porphyrins, and can be structurally modified using modular approaches.⁹ Initial results have also shown that with these building blocks we obtained more active catalysts with selectivities generally in between those of the non-encapsulated Rh-phosphine complex and the porphyrin-based capsule. The interaction between the Zn(salphen) building blocks and the

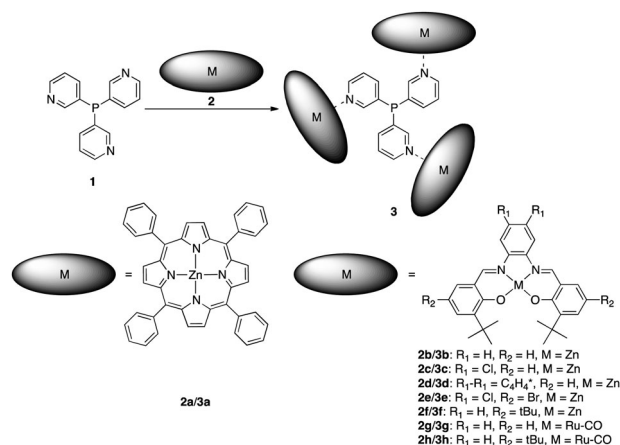
^a Department of Supramolecular and Homogeneous Catalysis, van 't Hoff Institute of Molecular Sciences, Science Park 904, 1098 XH Amsterdam, The Netherlands.
E-mail: j.n.h.reek@uva.nl; Fax: +31 20 525 5604; Tel: +31 20 525 5265

^b Department of Mechanical and Nuclear Engineering, Pennsylvania State University, 136 Research East, University Park, 16802 PA, USA

^c Bijvoet Centre for Biomolecular Research, Utrecht University, Padualaan 8, 3584 CH, Utrecht, The Netherlands

† Electronic supplementary information (ESI) available: Full data from catalysis results and full NMR spectra. CCDC 831697. For ESI and crystallographic data in CIF or other electronic format see DOI: 10.1039/c3cy20665c

‡ Current address: Institute of Chemical Research of Catalonia (ICIQ), Av. Països Catalans 16, 43007 Tarragona, Spain.



Scheme 1 The assembly of the porphyrin/salphen capsules assisted by the template-ligand, and a list of building blocks (i.e., 2–3) used in this paper.

pyridyl fragments of the phosphine template is stronger, which apparently did not translate to higher selectivities.

In this paper we provide insight into the origin of this difference supported by detailed investigations of the structure of the salphen-based capsules both in the solid state and in solution. Computational studies and solution-phase NMR have been used to show the conformational behaviour of these ligands in solution. This conformational flexibility of the encapsulated ligands affects the coordination environment around the transition metal centers, and ultimately the catalytic performance.

Results and discussion

Effects of the encapsulation by porphyrin or salphen units on hydroformylation catalysis

Before discussing the conformational behavior we will summarize the differences in catalytic behaviour observed for the capsules based on porphyrins and various zinc(II)salphen. In Tables 1–3 some of the previously reported results in the hydroformylation of various substrates (Scheme 2) using encapsulated catalysts based on several zinc-containing building blocks and the *meta*-trispyridylphosphine template are summarised.¹⁰ In addition, we carried out reactions with shorter reaction times such that the conversion indicates the relative reaction rate (Table 4).¹¹

Table 1 Results of the rhodium catalysed hydroformylation of 1-octene with trispyridylphosphine and the building blocks illustrated in Scheme 1^a

| Entry | Ligand | Yield ^b | TOF ^c | C1/C2 |
|----------------|---------------|--------------------|------------------|-----------|
| 1 ^d | 1 | 31 (6) | 5 (3) | 2.3 (2.9) |
| 2 ^e | 1 + 2a | 52 | 23 | 0.56 |
| 3 | 1 + 2b | 97 | 16 | 1.2 |
| 4 | 1 + 2c | 97 | 16 | 1.0 |
| 5 | 1 + 2d | 97 | 16 | 0.80 |
| 6 | 1 + 2f | 97 | 16 | 1.4 |

^a This table is compiled from various sources (ref. 8 and 10). All experiments were performed at 25 °C in toluene, with a substrate/catalyst ratio of 1052. The reaction time was 65 h except where noted. See Table S1 (ESI) for more details. ^b In percent. ^c Average TOF in (mol aldehyde) (mol Rh)^{−1} h^{−1}, based on conversion. ^d The numbers in brackets are for an experiment run for 24 h. ^e Reaction time: 24 h.

Table 2 Results of the rhodium catalysed hydroformylation of 2-octene with trispyridylphosphine and the building blocks illustrated in Scheme 1^a

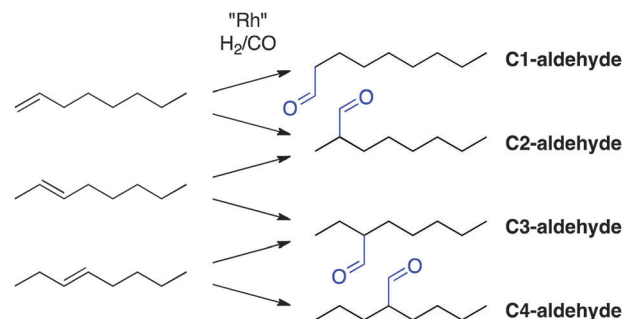
| Entry | Ligand | Yield ^b | TOF ^c | C2/C3 |
|-------|---------------|--------------------|------------------|-------|
| 1 | 1 | 17 | 2 | 1.3 |
| 2 | 1 + 2a | 32 | 5 | 0.11 |
| 3 | 1 + 2c | 47 | 7 | 1.0 |
| 4 | 1 + 2d | 48 | 7 | 0.86 |

^a This table is compiled from various sources (ref. 7 and 10). All experiments were performed at 25 °C in toluene, with a substrate/catalyst ratio of 1052. The reaction time was 73 h. See Table S1 (ESI) for more details. ^b In percent. ^c Average TOF in (mol aldehyde) (mol Rh)^{−1} h^{−1}, based on conversion.

Table 3 Results of the rhodium catalysed hydroformylation of 3-octene with trispyridylphosphine and the building blocks illustrated in Scheme 1^a

| Entry | Ligand | Yield ^b | TOF ^c | C3/C4 |
|-------|---------------|--------------------|------------------|-------|
| 1 | 1 | 26 | 4 | 0.98 |
| 2 | 1 + 2a | 45 | 6 | 0.31 |
| 3 | 1 + 2c | 60 | 9 | 1.0 |
| 4 | 1 + 2d | 63 | 9 | 0.98 |

^a This table is compiled from various sources (ref. 7 and 10). All experiments were performed at 25 °C in toluene, with a substrate/catalyst ratio of 1052. The reaction time was 73 h. See Table S1 (ESI) for more details. ^b In percent. ^c Average TOF in (mol aldehyde) (mol Rh)^{−1} h^{−1}, based on conversion.



Scheme 2 The rhodium-catalysed hydroformylation of octenes gives rise to several aldehyde products.

The difference between the non-encapsulated catalyst and the porphyrin-based capsule (entries 1 and 2 in Tables 1–3 respectively) is clear: the average TOF increases from 3 to 23 for 1-octene, and the C1/C2 product ratio changes from 2.9 to 0.56. Also for the internal octenes the activity increases (2–5), and a profound effect on the selectivity is observed. For 2-octene the C2/C3 ratio changes from 1.3 to 0.11, and for 3-octene the C3/C4 ratio changes from 0.98 to 0.31. This shows that the catalyst can distinguish between the carbon centers at the 3- and 4-position of the substrate (i.e., between an ethyl and an *n*-butyl group). This effect represents one of the unique examples of an unequalled selectivity induced by a nano-environment.¹²

When Zn(II)salphen are used for encapsulating the hydroformylation catalyst, the activity is in some cases still higher compared to the non-encapsulated ligands, as is apparent from the average TOFs reported in entries 1 and 3–6. From Table 4 it

Table 4 Results of the rhodium catalysed hydroformylation of 1-octene with trispyridylphosphine and the building blocks illustrated in Scheme 1^a

| Entry | Ligand | Yield ^b | TOF ^c | C1/C2 |
|----------------|---------------|--------------------|------------------|-------|
| 1 | 1 | 27 | 16 | 2.5 |
| 2 | 1 + 2b | 59 | 38 | 1.6 |
| 3 | 1 + 2c | 42 | 27 | 1.3 |
| 4 | 1 + 2e | 22 | 13 | 1.9 |
| 5 | 1 + 2f | 21 | 12 | 1.8 |
| 6 ^d | 1 + 2a | 44 | 126 | 0.60 |

^a All experiments were performed at 25 °C in toluene, with a substrate/catalyst ratio of 1000. The reaction time was 16 h. See Table S1 (ESI) for more details. ^b In percent. ^c Average TOF in (mol aldehyde) (mol Rh)⁻¹ h⁻¹, based on conversion. ^d Substrate/catalyst ratio was 5000, reaction time was 18 h.

can be seen that at short reaction times the average TOFs vary quite significantly when different salphen building blocks are applied. The TOFs range from 12 to 38, which means that the slowest encapsulated catalyst **2f** is slower than the non-encapsulated catalyst. However, none of the catalysts based on salphen building blocks converts 1-octene with a higher TOF than the porphyrin-based capsule. For the internal octenes, the salphen-based capsules are also slightly faster than the porphyrin-based ones with TOFs up to 7 for 2-octene and up to 9 for 3-octene. The selectivities are in between those of the non-encapsulated catalyst and the porphyrin-based capsule, ranging from 1.9 to 0.80 for 1-octene, and close to 1 for the internal octenes. Clearly, the encapsulation by the Zn(II)salphen leads to selectivities significantly different from those obtained with the Zn(II)porphyrin capsule. There is obviously a difference in the steric impediment upon capsule formation using the various building blocks. Here we further investigated the conformational fluxionality of the capsule based on the smaller Zn(II)salphen building blocks, and the consequence in coordination chemistry and catalysis.

Solid state structure

The assembly **3b** crystallized from a CH₂Cl₂–CH₃CN solution. Much to our surprise we found that the assembly exists in two different conformations, each being present in the unit cell. In one conformation all the pyridyl groups point up, so that the lone pairs of the pyridyl groups point in the same direction as that of the phosphorous center (designated as the “in” conformation). This causes the salphen units to encapsulate the phosphine (Fig. 1), similar to what molecular modelling suggested and what was found for the porphyrin encapsulated ligand. The other conformation has all the pyridyl groups pointing down (denoted as the “out” conformation), which makes the ligand very bulky, but the phosphorus donor atom is not encapsulated. It is clear that the capsule with the “in” conformation can only form monophosphine coordinated rhodium complexes, while in the “out” conformation maybe Rh–diphosphine complexes can be formed. In this way the conformation of the ligand directly influences the catalysis. It is also interesting to note that the conformation around zinc is different for the two complexes. In the “in” conformation the Zn ion resides 0.075(4) Å above the basal plane of the “close to square pyramidal” coordination environment around Zn

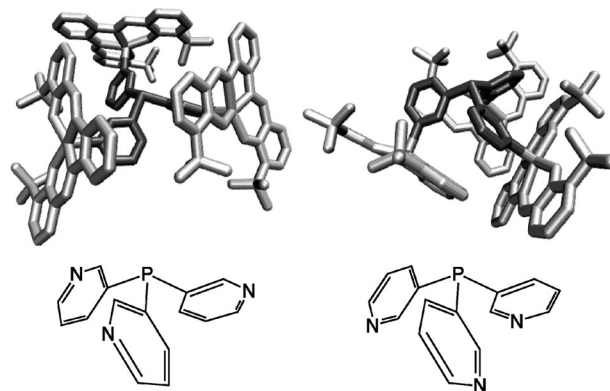


Fig. 1 The molecular structure of the tris-*meta*-pyridylphosphine/**3b** assembly exhibits two conformations. Left the “in” conformation, right the “out” conformation, and below line drawings of the different conformations of the central part of the assembly. In light gray the salphen units and in dark grey the trispyridylphosphine template. Selected bond distances (Å) and angles (°) with esd's in parentheses: P(1)–C(1) = 1.847(5), P(2)–C(38) = 1.827(4), Zn(1)–O(1) = 1.947(3), Zn(2)–O(3) = 1.971(3), Zn(1)–O(2) = 1.960(3), Zn(2)–O(4) = 1.959(3), Zn(1)–N(1) = 2.131(4), Zn(2)–N(4) = 2.114(3), Zn(1)–N(2) = 2.092(4), Zn(2)–N(5) = 2.071(3), Zn(1)–N(3) = 2.074(3), Zn(2)–N(6) = 2.105(3), C(1)–P(1)–C(1a) = 100.7(2), C(34)–P(2)–C(34c) = 103.3(2).

(86% of the Berry pseudo-rotation pathway between TP and SP). In the “out” conformation the Zn ion is located 0.069(4) Å above the basal plane (84%) defined by the N- and O donor atoms of the salphen ligand.¹³

It is sterically impossible for the porphyrin-based capsule to be in the “out” conformation according to molecular modelling. A recent X-ray molecular structure of the capsule based on tris-*meta*-pyridylphosphine and **3a** shows that it is only in the “in” conformation in the solid state.¹⁴ If these salphen based complexes are also able to adapt these out conformations in solution, this would provide a clear explanation for the different selectivities that these complexes induce. The difference in the solid-state structure can, however, be caused by packing effects, and does not necessarily represent the structures present in solution. Therefore, we next studied these supramolecular ligands in solution, to examine if this conformational flexibility actually plays a significant role.

Ru(II)salphen as analogues for Zn(II)salphen

From NMR titrations that were performed previously to establish the formation of assemblies of type **3** (Scheme 1), it is clear that the building blocks are in fast exchange on the NMR timescale despite a strong pyridyl–zinc interaction ($K_{\text{ass}} \sim 10^5 \text{ M}^{-1}$).^{8,9} NMR analysis of the Zn(II)salphen-based complexes therefore does not give any information about the conformational dynamics. Low-temperature NMR experiments of the Zn(salphen) based assemblies **3** (down to –90 °C) only give rise to a single set of ¹H NMR and ³¹P NMR signals. As at these temperatures the pyridyl–zinc complex is still in fast exchange on the NMR timescale, the single set of signals does not mean that co-existence of the two conformations (in and out) can be ruled out. Therefore, we have studied the conformational dynamics of these self-assembled capsules using Ru(II)salphen

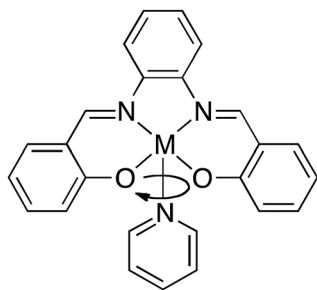


Fig. 2 The rotation of the pyridine ligand was calculated and compared between the Zn(II) and Ru(II)salphenes.

building blocks. Ru(II)salphen complexes¹⁵ are also known to form strong bonds with pyridines, and the exchange rates between coordinated and free pyridyl are slow on the NMR timescale. As the same salphen framework can be used, the size of the building block is very similar to Zn(II)salphenes. The Ru(II)salphenes have a CO coordinated opposite to the axial position of the pyridine donor, but since this will be on the outside of the capsule this will not interfere with the formation of capsule structure.

DFT calculations were performed to show the similarities and differences between the Zn(II)salphen-pyridyl and the Ru(II)salphen-pyridyl complexes. These calculations were performed using the B3LYP functional and the DGDZVP basis set.¹⁶ An energy profile was calculated for the rotation over the $N_{\text{pyr}}\text{-metal}$ bond (Fig. 2). In Fig. 3 the energy is shown as a function of the $O_{\text{sal}}\text{-M-N}_{\text{pyr}}\text{-C}_{\text{O,pyr}}$ torsion angle, and in Fig. 4 the length of the $N_{\text{pyr}}\text{-metal}$ bond is shown. The Zn-complex has its energy minimum when the pyridine plane is more or less parallel to the direction of the Zn-O bonds,¹⁷ and the bond length is intermediate at 2.16 Å. The energy barrier associated with this rotation is very small amounting to 0.5 kcal mol⁻¹. The Ru(II)-complex, however, has its global minimum when the pyridine plane is perpendicular to the O-O line, and a local minimum when it is parallel to this line. The bond length at the global minimum is 2.24 Å with a still relatively low rotational barrier of 3 kcal mol⁻¹. From these calculations it can be concluded that

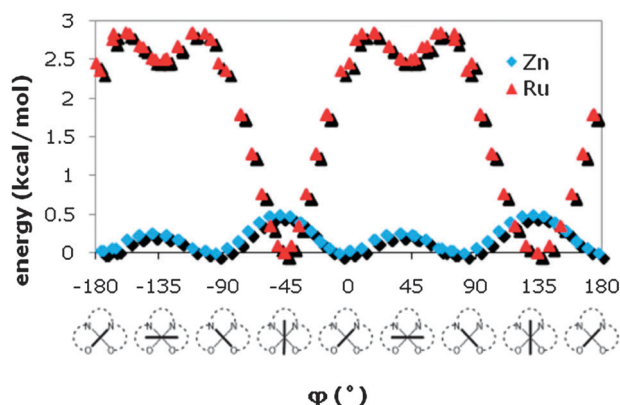


Fig. 3 The energy profile for the rotation of the pyridine ligand. In the x-axis the torsion angle $O\text{-M-N}_{\text{pyr}}\text{-C}_{\text{O,pyr}}$ φ is displayed.

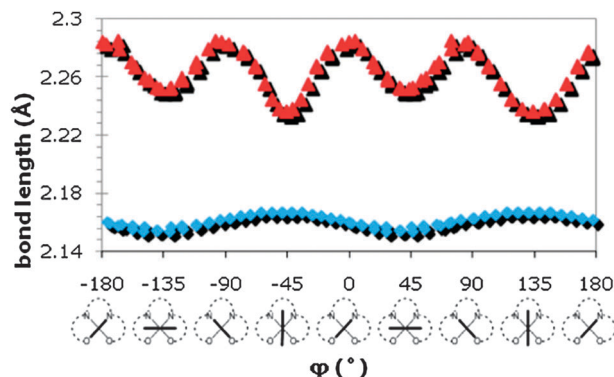


Fig. 4 The M-N_{pyr} bond length as a function of the torsion angle $O\text{-M-N}_{\text{pyr}}\text{-C}_{\text{O,pyr}}$ φ .

both complexes have virtually free rotation around the M-N_{pyr} bond. As the difference in the M-pyridyl distance is less than 0.1 Å the size and the shape of the capsule that is formed is virtually the same.

NMR analysis of Ru(II)salphen based complexes

NMR titrations were performed in d_8 -toluene with a fixed concentration of template-ligand **1** containing three pyridyl units (0.1 mM) and by gradually increasing the amount of **2g** or **2h** (0 to 0.3 mM).¹⁸ The ^1H and $^{31}\text{P}\{^1\text{H}\}$ spectra clearly demonstrate the slow exchange between the free and associated components. Separate peaks for the free phosphine, the 1 : 1 complex, the 2 : 1 complex and the 3 : 1 complex were observed, an observation also clearly visible in the ^{31}P NMR spectra (Fig. 6).

In the ^1H NMR spectra (Fig. 7) the aliphatic region shows distinct peaks for all these associated states because the *tert*-butyl groups shift upon coordination. Interestingly, the *tert*-butyl groups of salphen **2h** give two signals each in the 2 : 1 complex. This is not due to inequivalency of the salphenes but because the C_{2v} symmetry of the salphenes is broken in the 2 : 1 complex (see Fig. 5). In the 3 : 1 complex the C_{2v} symmetry is restored, and the *tert*-butyl groups give rise to only one peak. This means that the trispyridylphosphine template can be considered to have C_{3v} symmetry in all its forms: free, in the 1 : 1 complex, in the 2 : 1 complex, and even in the 3 : 1 complex. From this we can conclude that the symmetry inversion of the trispyridylphosphine unit is fast on the NMR timescale, even in its fully encapsulated form. If the inversion would be slow on the NMR timescale, we would observe the trispyridylphosphine as a C_3 symmetric entity, and the whole complex would have lower symmetry. Based on the simplicity of the NMR patterns we can also conclude that the salphenes can freely rotate around the Ru-N_{pyr} bond, in line with the energy barriers that we computed.

The signals in the aromatic region (see the ESI†) display the same symmetry for the various complexes: the 1 : 1 complex gives one set of signals for the salphen fragment, and two sets of signals (in a 1 : 2 ratio) for the pyridylphosphine. The 2 : 1 complex gives two sets of signals for the salphen groups and two sets of signals for the pyridylphosphine. And finally the 3 : 1 complex gives one set of signals for both the salphen and pyridylphosphine components.

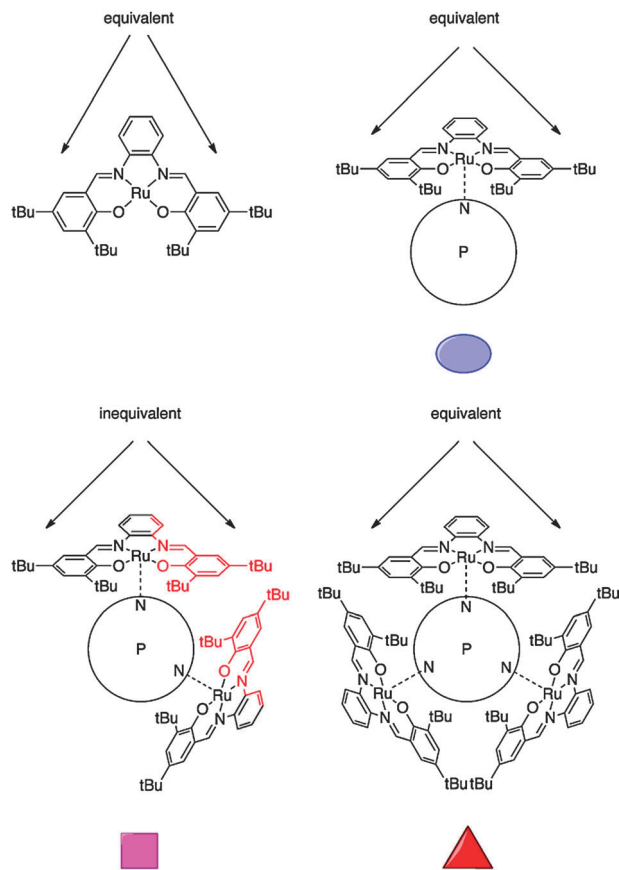


Fig. 5 The symmetry of the Ru(II)salphen is broken only in the 2 : 1 complex.

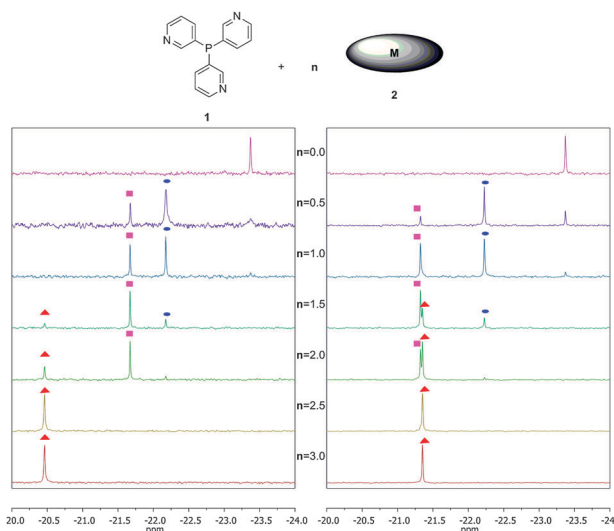


Fig. 6 $^{31}\text{P}\{^1\text{H}\}$ NMR spectra from the titration of **1** with **2h** (left) and **2g** (right). From top to bottom: 0, 0.5, 1, 1.5, 2, 2.5 and 3 equivalents of Ru(II)salphen are present.

Importantly, the free building blocks and the 1 : 1, 1 : 2 and 1 : 3 complexes can be distinguished by NMR as the Ru–pyridine exchange is slow on the NMR timescale. We expect substantial spectral differences if different capsular conformations are present,

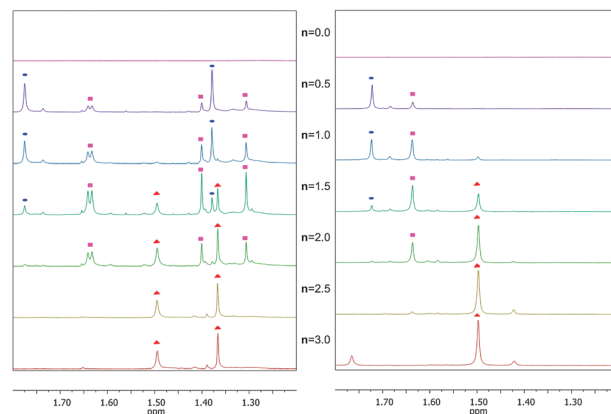


Fig. 7 ^1H NMR spectra (selected aliphatic region) from the titration of **1** with **2h** (left) and **2g** (right). From top to bottom: 0, 0.5, 1, 1.5, 2, 2.5 and 3 equivalents of Ru(II)salphen are present.

but we observe only one set of signals for the 3 : 1 complex. This indicates that either (1) only one conformation exists in solution, or (2) rapid interchange of different conformations occurs on the NMR timescale *via* a process that does not involve salphen dissociation. In the next section this non-dissociative conformational exchange using molecular dynamics is discussed.

Molecular dynamics modeling

The conversion between the “in” and the “out” conformation was studied by molecular dynamics simulations. As pyridyl decooordination may be required for this process, it is important to use a computational model that allows bond breaking. For this reason, we used the ReaxFF reactive force field¹⁹ method for these simulations. ReaxFF has been successfully applied in previous simulations on transition metal–organic interactions.^{19b,c} To enable application to the Ru–pyridine systems here we extended the ReaxFF C/O/N/H description, as developed for protein-based materials^{19d} with P–C, Zn–N and Ru–N bond- and angle parameters against a DFT-based training set, containing P–phenyl and P–CH₃ bonds, Ru–pyridine and Zn–NH₂ and Zn–NH₃ bond dissociation curves. The ReaxFF H/C/N/O parameters successfully reproduce rotational barriers in aromatic and non-aromatic hydrocarbons¹⁹ and heteroatoms^{19d} and provide a geometry-dependent charge-calculations, indicating that this method is suitable for studying complex rotational barriers in metallo-organic complexes, as described here.

In our molecular dynamics simulations we investigated three types of conformational changes, as shown in Fig. 8. The first is a so-called “propellor flip” (A) of the pyridylphosphine, which only changes the handedness of the pyridylphosphine propellor, but not the up or down orientation of the pyridyl groups. The second conformational change relates to the rotation of the salphen units around the N_{pyr}–Zn or N_{pyr}–Ru bond (B). These two types of rotation were performed as a benchmark, as these are known to be fast on the NMR timescale, thus providing a reference point.

Finally, and most importantly, we studied the pyridyl group rotation (C), which is necessary to go from the “in” to the “out”

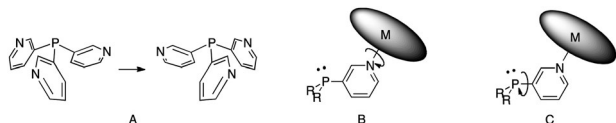


Fig. 8 The rotations that were investigated with ReaxFF molecular dynamics.

conformation. All these simulations were performed for both the “in” and the “out” conformation of the supramolecular assemblies based on the Zn complex **3b** and the Ru complex **3g**.

From Fig. 9 and 10 it can be deduced that for both the Zn and the Ru assembly the energy barrier for the propeller flip is much higher for the “out” conformation (35 and 80 kcal mol^{−1}, respectively) than for the “in” conformation (20 and 40 kcal mol^{−1}, respectively). The calculated energy barriers are higher than would be expected from the NMR measurements, as dynamic processes with barriers higher than 16–20 kcal mol^{−1} should be slow on the NMR timescale. This can be explained by a relatively short timescale used for the simulations (25 ps). While the complexes have plenty of time to equilibrate in the NMR experiment (nanosecond timescale), for example by rotation of the salphen units, this is not the case in the simulation. This can result in higher energy barriers for the simulations than in the experiments.²⁵ The relative barriers that are

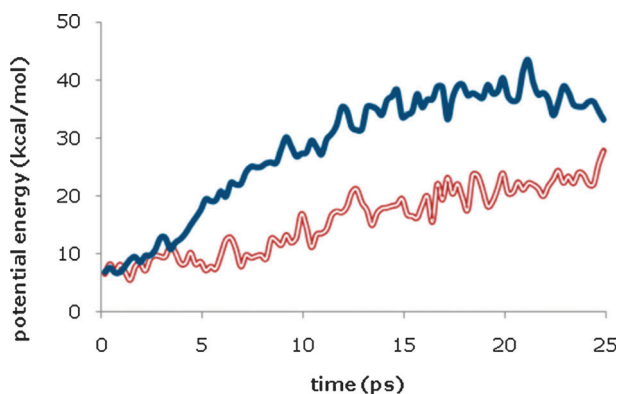


Fig. 9 Energy profile of the “propeller flip” (A) of complex **3b** starting from the “in” (red) and from the “out” conformation (blue) at $t = 0$.

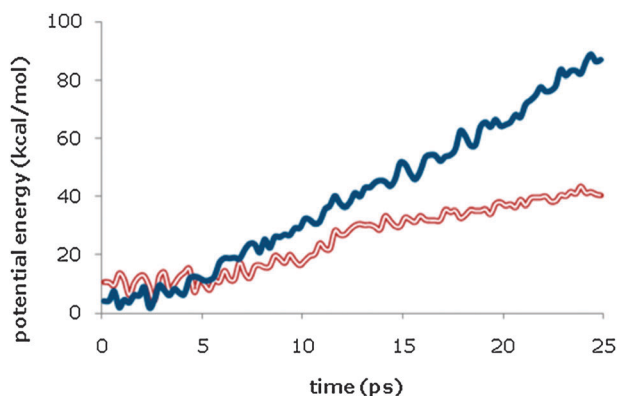


Fig. 10 Energy profile of the “propeller flip” (A) of complex **3g** starting from the “in” (red) and from the “out” conformation (blue) at $t = 0$.

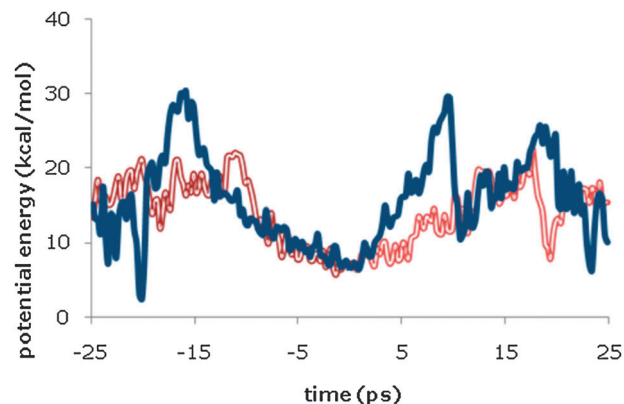


Fig. 11 Energy profile of the rotation of the salphen fragment (B) in the assembly based on complex **3b** starting from the “in” conformation (red) and from the “out” conformation (blue) at $t = 0$. Negative time signifies rotation in the opposite direction.

calculated can still be compared. Also for the salphen rotations (Fig. 11 and 12) relatively high barriers were found (up to 35 kcal mol^{−1} for the rotation of a Ru(II)salphen from the “out” conformation), whereas these rotations have also proven to be fast on the NMR timescale.

The barriers for pyridine rotation (Fig. 13 and 14) are in the order of 20 kcal mol^{−1}. Since this is lower than the barrier for the propeller flip, which is fast on the NMR timescale, we can conclude that the non-dissociative conformational exchange is also fast on the NMR timescale. This means that the supramolecular ligands **3b** and **3g** can exist as a mixture of conformations in solution, while the NMR spectra will give an average signal. Based on the current data we do not know the relative amount of each conformer in solution, and the calculations are not sufficiently accurate to predict the relative stability.

Metal complexes

The nature of the active species under hydroformylation conditions was previously determined directly using high-pressure infrared spectroscopy (HP-IR)²⁰ for the catalyst based on the

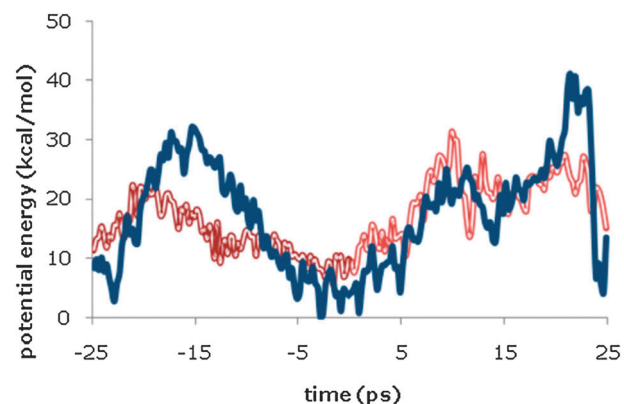


Fig. 12 Energy profile of the rotation of the salphen fragment (B) of the assembly based on complex **3g** starting from the “in” conformation (red) and from the “out” conformation (blue) at $t = 0$. Negative time signifies rotation in the opposite direction.

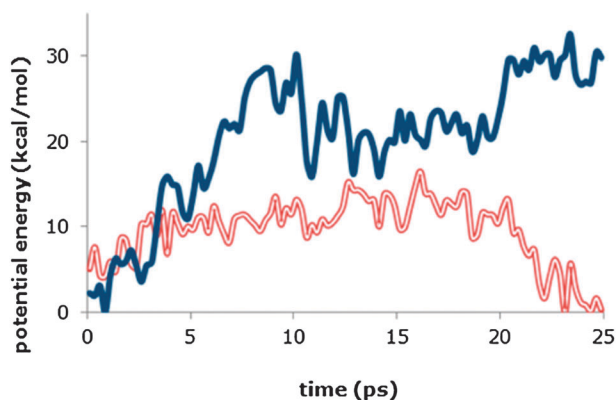


Fig. 13 Energy profile of the rotation of the pyridyl group with salphen attached (C) of complex **3b** (red) and **3g** (blue) starting from the "out" conformation at $t = 0$, ending up with the "in" conformation.

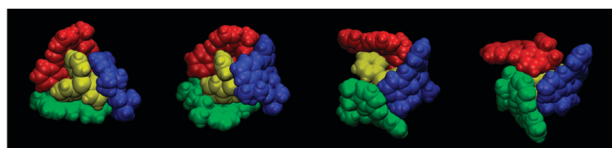


Fig. 14 Representation of the pyridyl group rotation of complex **3b**. Energy profile in Fig. 13.

porphyrin capsule comprising **3a**.⁶ In HP-IR three distinct bands were observed in the carbonyl-stretching region. This means that a monophosphine–rhodium species is formed, which is in line with the HP NMR data and the distinct catalytic properties. For catalysts based on the salphen capsule, only indirect evidence of mono-phosphine species has been reported so far.⁸ In previous studies of the catalyst precursor it has been shown that a 2 : 1 mixture of **3f** and $\text{Rh}(\text{acac})(\text{CO})_2$ in CDCl_3 gives rise to two signals in the ^{31}P NMR: a singlet at -20.9 ppm (free ligand), and a doublet at 43.4 ppm with a coupling constant of 182 Hz, which is characteristic for a monophosphine–Rh complex.

We also recorded the HPIR spectrum under actual hydroformylation conditions, which shows the typical bands observed for a mixture of complexes with two phosphorus donor atoms in the ee and ea coordination mode (Fig. 15). The HP-IR spectrum can be simulated¹⁶ relatively well by making a 1 : 1 : 1 linear combination of the equatorial–axial and equatorial–equatorial bis-phosphine complexes and the equatorial monophosphine complex (Fig. 16). In combination with the molecular modeling studies that show rapid exchange between "in" and "out" conformations, we conclude that it is most likely that these salphen-based catalysts are able to adopt "out" conformations upon coordination that do not exclusively enforce formation of mono-phosphine complexes.

Conclusions

By a combination of X-ray analysis, spectroscopic analysis, DFT and ReaxFF molecular dynamics calculations we have been able

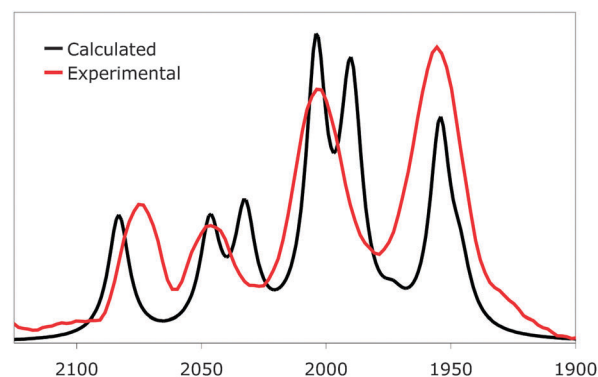


Fig. 15 HPIR of the active species in hydroformylation when using **3f** as the ligand.

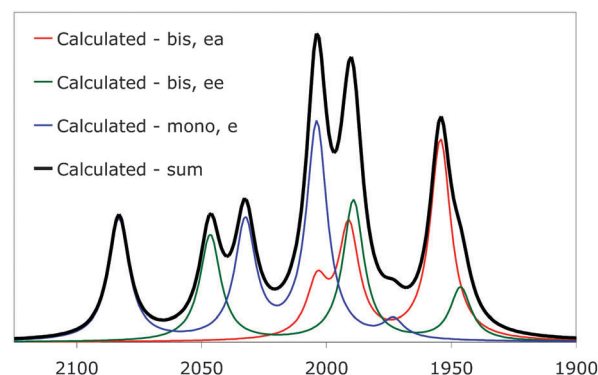


Fig. 16 The simulated IR spectrum of the Rh-hydroformylation catalyst based on **3f** is a 1 : 1 : 1 linear combination of the ea and ee bis-phosphine complexes and the equatorial mono-phosphine complex.

to determine that complexes of type **3** most likely exist as multiple conformations both in solution and in the solid state. Whereas the porphyrin based assemblies were found in only one conformation in which the phosphorus donor atom was shielded by the porphyrins, the salphen based analogues can also adapt a conformation in which the phosphorus donor atom is much less shielded. The consequences for coordination chemistry are large, as for the porphyrins we found that the shielding resulted in exclusive mono-phosphorus coordination complexes,⁶ whereas for the salphen based assemblies bis-phosphorus complexes are also formed. Although in these complexes the metal is also shielded by the salphens,^{9c} the activity and selectivity is very different from the encapsulated mono-phosphine rhodium complexes. Further exploration of the salphen framework might result in a structure that does share this ability with the porphyrins, although a valid question is whether this salphen would be as synthetically accessible as the easily prepared parent $\text{Zn}(\text{II})$ tetraphenylporphyrin. More interestingly, chiral versions of these salphen or porphyrin-based capsules are an attractive target for future directions in this area.

Notes and references

- (a) M. Fujita, K. Umemoto, M. Yoshizawa, N. Fujita, T. Kusakawa and K. Biradha, *Chem. Commun.*, 2001, 509;

- (b) J. Rebek Jr., *Angew. Chem., Int. Ed.*, 2005, **44**, 2068; (c) F. Hof, S. L. Craig, C. Nuckolls and J. Rebek Jr., *Angew. Chem., Int. Ed.*, 2002, **41**, 1488; (d) M. M. Conn and J. Rebek Jr., *Chem. Rev.*, 1997, **97**, 1647; (e) J. M. Lehn, *Science*, 1985, **227**, 849.
- 2 (a) *Supramolecular catalysis*, ed. P. W. N. M. Van Leeuwen, Wiley-VCH, Weinheim, 2008; (b) T. S. Koblenz, J. Wassenaar and J. N. H. Reek, *Chem. Soc. Rev.*, 2008, **37**, 247; (c) J. I. Van der Vlugt, T. S. Koblenz, J. Wassenaar and J. N. H. Reek, *Chemistry in Self-Assembled Nanoreactors*, in *Molecular Encapsulation: Organic Reactions in Constrained Systems*, ed. U. H. Brinker and J.-L. Miesusset, John Wiley & Sons, Ltd., Chichester, UK, 2010, pp. 145–174; (d) D. M. Vriezema, M. C. Aragonés, J. A. A. W. Elemans, J. J. L. M. Cornelissen, A. E. Rowan and R. J. M. Nolte, *Chem. Rev.*, 2005, **105**, 1445; (e) D. Fiedler, D. H. Leung, R. G. Bergman and K. N. Raymond, *Acc. Chem. Res.*, 2005, **38**, 349; (f) D. H. Leung, R. G. Bergman and K. N. Raymond, *J. Am. Chem. Soc.*, 2006, **128**, 9781; (g) D. H. Leung, R. G. Bergman and K. N. Raymond, *J. Am. Chem. Soc.*, 2007, **129**, 2746.
- 3 M. Fujita, D. Oguro, M. Miyazawa, H. Oka, K. Yamaguchi and K. Ogura, *Nature*, 1995, **378**, 469; T. Kusakawa and M. Fujita, *Angew. Chem., Int. Ed.*, 1998, **37**, 3142–3144; D. L. Caulder, R. E. Powers, T. N. Parac and K. N. Raymond, *Angew. Chem., Int. Ed.*, 1998, **37**, 1840; C. J. Hastings, M. D. Pluth, R. G. Bergman and K. N. Raymond, *J. Am. Chem. Soc.*, 2010, **132**, 6938.
- 4 M. Pluth, R. Bergman and K. Raymond, *Science*, 2007, **316**, 85.
- 5 M. Yoshizawa, M. Tamura and M. Fujita, *Science*, 2006, **312**, 251.
- 6 (a) V. F. Slagt, J. N. H. Reek, P. C. J. Kamer and P. W. N. M. van Leeuwen, *Angew. Chem., Int. Ed.*, 2001, **40**, 4271; (b) V. F. Slagt, P. C. J. Kamer, P. W. N. M. van Leeuwen and J. N. H. Reek, *J. Am. Chem. Soc.*, 2004, **126**, 1526; (c) V. F. Slagt, P. W. N. M. van Leeuwen and J. N. H. Reek, *Angew. Chem., Int. Ed.*, 2003, **42**, 5619; (d) J. Flapper and J. N. H. Reek, *Angew. Chem., Int. Ed.*, 2007, **46**, 8590; (e) T. S. Koblenz, H. L. Dekker, C. G. De Koster, P. W. N. M. van Leeuwen and J. N. H. Reek, *Chem. Commun.*, 2006, 1700; (f) T. S. Koblenz, H. L. Dekker, C. G. De Koster, P. W. N. M. van Leeuwen and J. N. H. Reek, *Chem.-Asian J.*, 2011, **6**, 2431; (g) T. S. Koblenz, H. L. Dekker, C. G. De Koster, P. W. N. M. van Leeuwen and J. N. H. Reek, *Chem.-Asian J.*, 2011, **6**, 2444.
- 7 M. Kuil, PhD thesis, University of Amsterdam, 2006.
- 8 A. W. Kleij, M. Lutz, A. L. Spek, P. W. N. M. van Leeuwen and J. N. H. Reek, *Chem. Commun.*, 2005, 3661.
- 9 (a) A. W. Kleij, M. Kuil, D. M. Tooke, M. Lutz, A. L. Spek and J. N. H. Reek, *Chem.-Eur. J.*, 2005, **11**, 4743; (b) A. W. Kleij, D. M. Tooke, A. L. Spek and J. N. H. Reek, *Eur. J. Inorg. Chem.*, 2005, 4626; (c) V. Bocokic, M. Lutz, A. L. Spek and J. N. H. Reek, *Dalton Trans.*, 2012, 3740.
- 10 A. M. Kluwer, I. Ahmad and J. N. H. Reek, *Tetrahedron Lett.*, 2007, **48**, 2999.
- 11 Hydroformylation experiments were performed in a stainless steel autoclave with an insert for GC vials to run up to 15 experiments at the same time. The autoclave was equipped with a pressure indicator, and was kept at constant room temperature in an oil bath. Each GC vial was equipped with a stirring bar. In a typical run each GC vial contained 1 ml of a solution of Rh(acac)(CO)₂ (0.1 mM), meta-trispyridylphosphine (9 eq.), Zn(II)salphen (27 eq.) and octene (1000 eq.). In the cases where salphens were used as an associated building block, diisopropyl-ethylamine (2.5 eq.) was used to protect the salphens from acid-induced autocatalytic demetallation.
- 12 M. Kuil, T. Soltner, P. W. N. M. van Leeuwen and J. N. H. Reek, *J. Am. Chem. Soc.*, 2006, **128**, 11344.
- 13 Crystal structure determination of **3b**: C₉₉H₁₀₂N₉O₆PZn₃, *F*_w = 1741.04, orange block, 0.22 × 0.2 × 0.14 mm³, trigonal crystal system, space group *P* $\bar{3}$ c1, cell parameters: *a* = 20.8644(4) Å, *c* = 52.9489(13) Å, *V* = 19961.8(7) Å³, *Z* = 8, 204 945 reflections were measured on a Nonius KappaCCD diffractometer with a rotating anode and MoK α radiation (graphite mono-chromator, λ = 0.71073 Å) at a temperature of 150(2) K. A multi-scan absorption correction was applied (μ = 0.784 mm^{−1}, 0.68–0.9 transmission). 8702 unique reflections (*R*_{int} = 0.0974), of which 7387 were observed [*I* > 2 σ (*I*)]. The structure was solved with the program DIRDIF,²¹ and refined using the program SHELXL-97²² against *F*² of all reflections up to a resolution of θ = 22.48°. Non-hydrogen atoms were freely refined with anisotropic displacement parameters. H atoms were placed at geometrically idealized positions [*d*(C–H) = 0.98 for methyl H atoms and 0.95 for other H atoms] and constrained to ride on their parent atoms, with *U*_{iso}(H) = 1.5*U*_{eq}(C) for methyl H atoms and *U*_{iso}(H) = 1.2*U*_{eq}(C) for all other H atoms. The structure contained disordered solvent molecules, which were taken into account by back-Fourier transformation with PLATON/SQUEEZE,²³ (SQUEEZE volume = 4202 Å³, recovered number of electrons = 502). 722 refined parameters, 0 restraints. *R* (obs. refl.): *R*₁ = 0.0538, *wR*₂ = 0.1105. *R* (all data): *R*₁ = 0.0746, *wR*₂ = 0.1185. Weighting scheme *w* = 1/[$\sigma^2(F_o^2)$ + (0.0367*P*)² + 1.1877*P*], where *P* = (*F*_o² + 2*F*_c²)/3. GoF = 1.179. Residual electron density between −0.394 and 0.387 e Å^{−3}. Checking for additional symmetry was performed with the program PLATON.²⁴ CCDC 831697.
- 14 V. Bocokić, A. Kalkan, M. Lutz, A. L. Spek, D. Gryko and J. N. H. Reek, Submitted.
- 15 K. Chichak, U. Jacquemard and N. R. Branda, *Eur. J. Inorg. Chem.*, 2002, 357.
- 16 M. J. Frisch, G. W. Trucks, H. B. Schlegel, G. E. Scuseria, M. A. Robb, J. R. Cheeseman, J. A. Montgomery Jr., T. Vreven, K. N. Kudin, J. C. Burant, J. M. Millam, S. S. Iyengar, J. Tomasi, V. Barone, B. Mennucci, M. Cossi, G. Scalmani, N. Rega, G. A. Petersson, H. Nakatsuji, M. Hada, M. Ehara, K. Toyota, R. Fukuda, J. Hasegawa, M. Ishida, T. Nakajima, Y. Honda, O. Kitao, H. Nakai, M. Klene, X. Li, J. E. Knox, H. P. Hratchian, J. B. Cross, C. Adamo, J. Jaramillo, R. Gomperts, R. E. Stratmann, O. Yazyev, A. J. Austin, R. Cammi, C. Pomelli, J. W. Ochterski, P. Y. Ayala, K. Morokuma, G. A. Voth,

- P. Salvador, J. J. Dannenberg, V. G. Zakrzewski, S. Dapprich, A. D. Daniels, M. C. Strain, O. Farkas, D. K. Malick, A. D. Rabuck, K. Raghavachari, J. B. Foresman, J. V. Ortiz, Q. Cui, A. G. Baboul, S. Clifford, J. Cioslowski, B. B. Stefanov, G. Liu, A. Liashenko, P. Piskorz, I. Komaromi, R. L. Martin, D. J. Fox, T. Keith, M. A. Al-Laham, C. Y. Peng, A. Nanayakkara, M. Challacombe, P. M. W. Gill, B. Johnson, W. Chen, M. W. Wong, C. Gonzalez and J. A. Pople, *Gaussian 03, Revision C.02*, Gaussian, Inc., Wallingford, CT, 2004.
- 17 Compare also with: E. C. Escudero-Adan, J. Benet-Buchholz and A. W. Kleij, *Eur. J. Inorg. Chem.*, 2009, 3562.
 - 18 NMR measurements were recorded on a Varian 500 NMR spectrometer. The titration experiments were performed as follows: a sample containing 0.75 ml of a solution of 0.1 mM tris-*m*-pyridylphosphine in d_8 -toluene was prepared, and measured. To this sample, 0.1 ml of a solution of Ru(II)salphen (0.375 mM) and tris-*meta*-pyridylphosphine (0.1 mM) was added for each successive measurement.
 - 19 ReaxFF MD calculations were performed with the stand alone ReaxFF program: (a) A. C. T. van Duin, S. Dasgupta, F. Lorant and W. A. Goddard, *J. Phys. Chem. A*, 2001, **105**, 9396. Force field parameters can be obtained from Adri van Duin (acv13@psu.edu) upon request. For some examples see: (b) K. Chenoweth, A. C. T. van Duin, P. Persson, M. J. Cheng, J. Oxgaard and W. A. Goddard, *J. Phys. Chem. C*, 2008, **112**, 14645; (c) A. C. T. van Duin, V. S. Bryantsev, M. S. Diallo, W. A. Goddard, O. Rahaman, D. J. Doren, D. Raymand and K. Hermansson, *J. Phys. Chem. A*, 2010, **114**, 9507; (d) O. Rahaman, A. C. T. van Duin, W. A. Goddard III and D. J. Doren, *J. Phys. Chem. B*, 2011, **115**, 249; (e) K. Chenoweth, A. C. T. van Duin and W. A. Goddard, *J. Phys. Chem. A*, 2008, **112**, 1040–1053; (f) M. Aryanpour, A. C. T. van Duin and J. D. Kubicki, *J. Phys. Chem. A*, 2010, **114**, 6298–6307. The simulations were performed using the sliding torsion restraint method, which essentially slowly progresses selected torsion angles (see figures in the text) during a MD/NVT ($T = 250$ K) simulation. This is similar to the umbrella sampling concept – essentially allowing the system to respond to a perturbation by performing a molecular dynamics simulation.
 - 20 High-pressure FT-IR was performed in a stainless steel 50 ml autoclave equipped with INTRAN windows (ZnS), a mechanical stirrer and a pressure transducer. The spectra were recorded with a Nicolet 510 FT-IR spectrophotometer. The high-pressure infrared experiments were performed in a high-pressure infrared autoclave that was degassed and filled with argon before use. In a typical experiment P(*meta*-pyr)₃ (95 μ mol, 25 mg) and ZnTPP (284 μ mol, 192 mg) in DCM (13 ml) were injected into the autoclave. The autoclave was flushed three times with syngas, and pressurized to 20 bar. The background spectrum was taken from this mixture. Rh(acac)(CO)₂ (11 μ mol, 2.6 mg) in DCM (1 ml) was injected *via* the injection chamber. The catalyst was left to incubate for one hour, during which spectra could be recorded. 1-Octene (2.1 mmol, 330 μ l) in DCM (1 ml) was injected *via* the injection chamber, after which more spectra could be recorded.
 - 21 P. T. Beurskens, G. Admiraal, W. P. Bosman, S. Garcia-granda, R. O. Gould, J. M. M. Smits and S. Smykalla, *The DIRDIF Program System*, University of Nijmegen, The Netherlands.
 - 22 G. M. Sheldrick, *Acta Crystallogr., Sect. A: Fundam. Crystallogr.*, 2008, **A64**, 112.
 - 23 P. van der Sluis and A. L. Spek, *Acta Crystallogr., Sect. A: Fundam. Crystallogr.*, 1990, **A46**, 194.
 - 24 A. L. Spek, *J. Appl. Crystallogr.*, 2003, **36**, 7.
 - 25 These simulations probably overestimate the rotation barrier, since the system is given only a limited time to respond to the sliding torsion perturbation. Increasing the temperature would give better sampling, but this also increases the temperature noise, making the measured barrier less accurate.